Vertical Wind Disturbances in the Troposphere and Lower Stratosphere Observed by the MU Radar

KAORU SATO

Department of Geophysics, Faculty of Science, Kyoto University, Kyoto, Japan

(Manuscript received 31 July 1988, in final form 26 June 1990)

ABSTRACT

An analysis is made of vertical wind disturbances (VWDs) observed by the MU radar (Shigaraki, Shiga, Japan) in terms of the wave structures, sources, and vertical momentum flux. First, it is shown through spectral and lag-correlation analyses that there are several common features in three observation periods when the VWDs appeared: large power in the vertical wind fluctuations exists below a height of ~20 km and is distributed largely at lower frequencies. The decrease in power near 20 km is sharp and the correlation between vertical winds above and below the level is very small, suggesting that the height of 20 km is a special level for the VWDs such as a critical level. The disturbances below 20 km consist of several modes in a height-frequency space, some of which oscillate almost in phase in a wide height range spanning ~8 km at the maximum.

Second, using eight sets of the MU radar data, the relationship between vertical wind activity and horizontal wind near the surface is examined in order to identify the source of the VWDs. The activity of the vertical wind is closely related to both direction and strength of the horizontal wind near the surface at Yonago (about 250 km west of Shigaraki). This indicates that the VWDs are due mainly to gravity waves generated by the effect of topography with heights of ~1000 m located between Yonago and Shigaraki. The features obtained through the wave structure analysis can be interpreted well as characteristics of topographically forced waves.

Finally, vertical momentum flux associated with the VWDs is examined. Although it is generally difficult to examine the vertical momentum flux associated with quasi-stationary mountain waves from observations at one location, the estimation is possible to some extent when the spatial phase fluctuates largely according to temporal changes of the background wind. As a result, some of the VWDs' characteristics on the momentum flux consistent with the view of mountain waves are obtained.

1. Introduction

The VHF Doppler clear-air radar is a powerful tool to examine small-scale disturbances like gravity waves with accuracy of about 0.1 m s^{-1}, since the wind measurement has fine vertical and time resolution. One of the advantages of the VHF radar observation is the ability to measure vertical wind directly. Using the VHF radars, large disturbances of vertical wind recurring at a several-day period in the troposphere and lower stratosphere were detected at various locations: Poker Flat, Alaska; the lee of the Colorado Rockies; and the Rhone Delta, Southern France (Ecklund et al. 1981, 1982, 1985). In these studies, large differences in the shape of the frequency power spectra of vertical wind fluctuation were indicated between the periods with and without the VWDs. From observation of the large correlation between the zonal wind at 500 mb and the vertical wind activity, and of the stronger power at a site nearer mountains relative to one in flat terrain, Ecklund et al. (1982) suggested that the VWDs were generated by the topographic effect.

VWDs are also occasionally observed by the MU radar at Shigaraki, Japan, mainly in late autumn and winter (Ohno 1988). Ohno made a preliminary analysis of the VWDs using the wind data obtained by the MU radar in January 1986. He showed that a strong turbulent layer with a vertical width of 1–2 km was located near 18 km during the period with the VWDs, which is similar to the lee wave observation with aircraft at the Colorado Rockies by Lilly and Kennedy (1973). The turbulent layer tilted a little zonally but not meridionally, suggesting that the VWDs have small zonal scales. Ohno compared the vertical winds obtained directly from a vertical beam (w_v) with those estimated from two pairs of two symmetrical beams around the zenith tilted zonally (w_z) and meridionally (w_m), assuming homogeneity of the wind field between the beams. As a result, it was found that w_v and w_m are almost the same while w_v is largely different from w_z. This is consistent with the zonal tilt of the turbulent layer. He found that in some periods with the VWDs, the vertical profiles of horizontal wind at heights of 5–22 km obtained by the MU radar observations resemble

Corresponding author address: Dr. Kaoru Sato, Dept. of Geophysics, Faculty of Science, Kyoto University, Kyoto 606, Japan.

each other. Thus, he suggested a possibility that the VWDs observed by the MU radar are caused by a topographic effect because the vertical and horizontal propagation of the waves must be closely connected with the horizontal wind profile.

However, the detailed vertical structure of VWDs has not yet been examined. Thus we make an analysis using several datasets obtained with the MU radar (when VWDs were present) in order to investigate common features of the VWDs. Moreover, there is no convincing evidence that the VWDs observed with the MU radar are due to topographically forced waves. No such high mountains as the Rocky Mountains exist around the MU radar. Thus, we make an examination of the relationship between the activity of vertical wind and horizontal wind near the surface.

This study also describes some of the characteristics on vertical momentum flux associated with the VWDs. Vertical momentum flux can be estimated directly from the wind data with high resolution using the VHF radars (Vincent and Reid 1983). VanZandt et al. (1990) made a velocity azimuth display (VAD) measurement in March 1986 using the MU radar and pointed out anisotropy of the velocity fluctuation field in the lower stratosphere. Using the same data, Fritts et al. (1990) showed that the anisotropy is consistent with the bias of the wavenumber vector deduced from the vertical momentum flux. However, Vincent and Reid's method cannot be applied to the stationary mountain waves because it is difficult to discriminate the waves from the background wind in observation data at a single location. Therefore, in this study the examination on vertical momentum flux associated with the VWDs is made assuming that the observed wind fluctuations are due to phase fluctuations of the quasi-stationary waves.

Section 2 presents a detailed description of the data. The characteristics of mean wind for observations with and without VWDs are shown in section 3. The vertical structure of the VWDs is examined in section 4. The correlation of the activity of vertical wind with the horizontal wind near the surface is analyzed in section 5. In section 6, the vertical momentum flux associated with the VWDs is examined. Concluding remarks are made in section 7.

2. Data description and method of analysis

Eight sets of wind data for the troposphere and lower stratosphere obtained in late autumn and winter using the MU radar are analyzed (Table 1). The observed height range is around 5–25 km with a spatial resolution of 150 or 300 m along the beam direction. The time resolution is 1–9 minutes. Although beam configurations for the observations are different from each other, we use the data of radial velocities measured by five beams, directed vertically, and tilted to the east, west, north, and south with the same zenith angles of 10°. The resolution of radial wind velocity is less than 0.1 m s^{-1} when signal-to-noise ratio of the echo is sufficiently high. Details of the system of the MU radar are described by Fukao et al. (1985a,b).

TABLE 1. Parameters of observations.

	Date	Observation period (h)	Time resolution (min)	Height resolution (m)
A	6–8 Nov 1985	31.4	8.2	300
B	13–14 Nov 1985	23.0	1.2	150
C	16–17 Dec 1985	20.9	1.1	150
D	6–10 Jan 1986	98.2	2.5	150
E	22–24 Jan 1986	47.4	7.5	300
F	28–29 Jan 1986	21.1	1.1	150
G	26–28 Jan 1987	47.6	1.1	150
H	15–17 Dec 1987	48.8	9.1	300
	Total	338.4		

An example of time series of the vertical wind component in an observation period D is shown as a function of height in Fig. 1. The increase in vertical wind fluctuations after approximately 48 hours suggests that the period D be divided into two halves (hereafter referred to as D_1 and D_2). While there is small variation in D_1, large disturbances occasionally exceeding 3 m s^{-1} are found in D_2. Following Ecklund et al. (1981, 1982, 1985, 1986), hereafter we refer to such periods with small vertical wind variation similar to D_1 as "*quiet*" periods and those with large disturbances of vertical wind similar to D_2 as "*active*" periods.

In order to investigate the vertical structures and vertical momentum flux associated with the VWDs in detail, several cases are analyzed in sections 4 and 6 for active and quiet periods out of the observations of A–H shown in Table 1. We choose B, C, and D_2 as active periods, and A, D_1, and G as quiet periods, during which the activity of vertical wind is almost uniform and the number of missing data is small. On the other hand, all observation data presented in Table 1 are used in section 5 to investigate the relationship between the activity of vertical wind and the horizontal wind near the surface.

For analysis of gravity waves whose intrinsic high-frequency cutoff is the Brunt-Väisälä frequency of (5–10 min)$^{-1}$ in the troposphere and lower stratosphere, such a high time resolution as 1 min is not needed. Since the number of data is very large for B, C, and G, components having a period less than 5 min were removed by passing the original data through a lowpass filter, and the filtered data were sampled every 2.5 min corresponding to the new Nyquist frequency. Similarly for D, time series including components with periods larger than 10 min sampled every 5 min were used. However, the time resolution is not critical for the analyses made in this study because the VWDs primarily have large power at lower frequencies as is shown in section 4.

3. Vertical structure of the mean wind

Figure 2 presents vertical profiles of the time-mean wind in the active and quiet periods. While various structures of the horizontal wind exist in the quiet periods, the structures in the active periods have some similar features; i.e., a westerly jet located at a height of 11–14 km and positive meridional wind of about one-half the magnitude of the zonal component. However, we cannot attribute the cause of the VWDs directly to the horizontal wind structure, since a similar structure is observed for a quiet period D_1.

It is also worth noting that the mean vertical wind is large in the active periods, indicating the presence of components with large power having long periods comparable to the observation periods of 20–50 hours. The mean vertical wind is large below about 20 km with a vertical scale compression from about ten to a few kilometers where a large vertical shear of the horizontal mean wind exists above the subtropical westerly jet. The horizontal mean wind is near zero at the height of about 20 km. This suggests that the quasi-stationary component is due to topographically excited gravity wave motions. However, the mean vertical wind in the quiet periods is small and does not have such characteristics seen in the active periods.

Further analysis for the mean vertical wind component in the active periods cannot be made directly. Since it is difficult to extract the horizontal wind component of the quasi-stationary waves from the background wind with a similar large vertical scale using any time and/or spatial filtering, we cannot examine characteristics such as the polarization relation, which is important for determination of physical processes causing the large mean vertical wind. However, it is possible to examine this issue indirectly. The spatial phase of topographically forced waves varies temporally following small temporal changes in the background wind—because horizontal wavelengths of the waves should be small. The temporal variations of the spatial phase are observed with other temporally oscillating waves as fluctuations at one location. Thus, the analysis of the fluctuating components could provide useful information for the examination of quasi-stationary waves, although it is generally difficult for observations at one location to separate these different types of waves.

4. Vertical structure of the disturbances

In this section we use w_v (vertical winds obtained using a vertical beam) for the analysis, because w_v are estimated without any assumption. Hereafter w_v is referred to as w. First, we examine the VWDs in terms of the difference in the power of vertical wind fluctuations between active and quiet periods as a function of height. Figure 3 shows the vertical profiles of variance of w and those weighted by air density adopted from the U.S. Standard Atmosphere 1976. The variances in the active periods are very large compared with the quiet periods. It is noted that the vertical wind fluctuations are larger than the amplitudes observed in vertical profiles of the mean vertical wind in the active periods (see Fig. 2). The variances of w weighted by

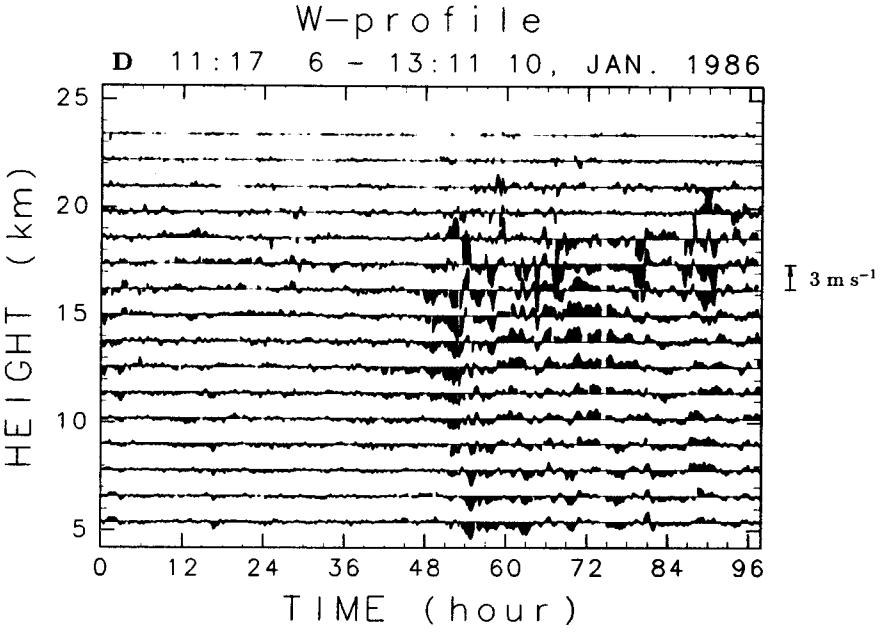

FIG. 1. The vertical wind profile as a function of height measured with the vertical beam during 6–10 January 1986. The spacing of horizontal lines shows velocity of 3 m s^{-1}. Errors in wind are less than 0.1 m s^{-1}.

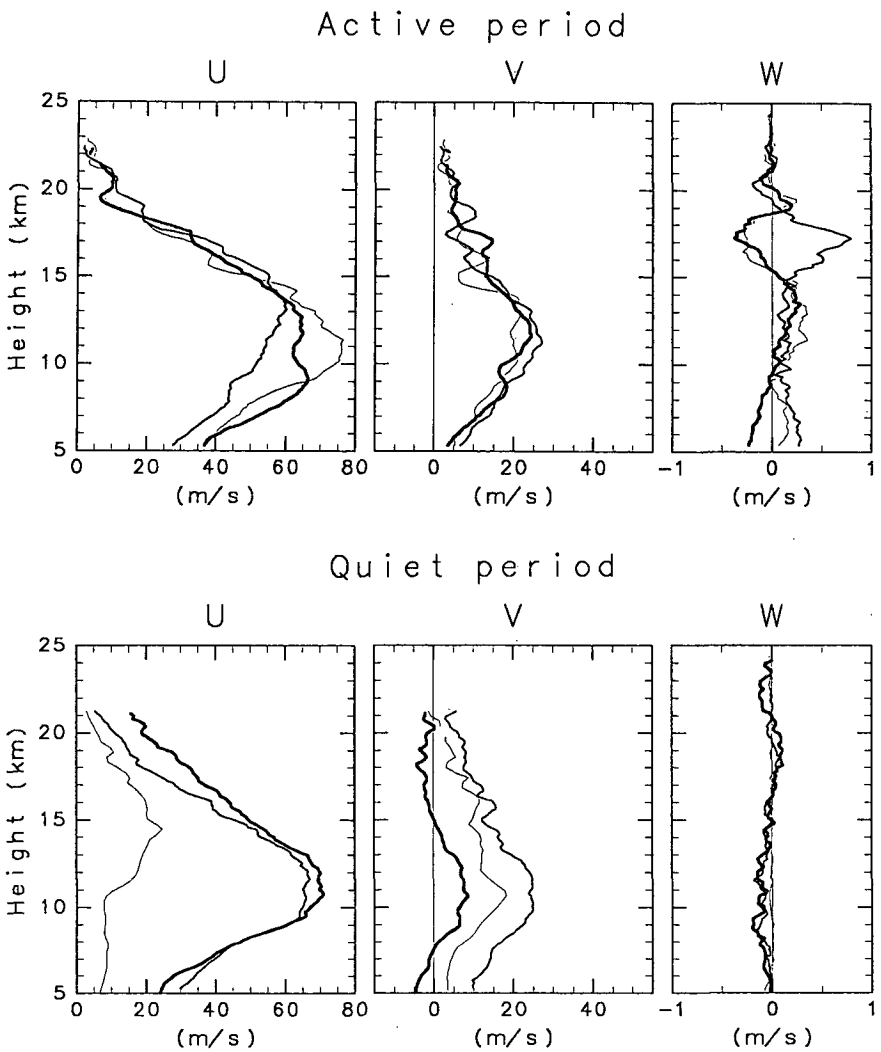

FIG. 2. Vertical profiles of each component of the time mean wind in active (top) and quiet (bottom) periods as a function of height. Thick, thin, and very thin lines for active periods show the profiles of D_2, C, and B, respectively. Thick, thin, and very thin lines for quiet periods show the profiles of G, D_1, and A, respectively.

air density for the active periods have a characteristic vertical structure: a gradual decrease in a height range of 5–11 km, an increase above 11 km to a peak at 17–18 km, and a sharp decrease above the peak. The figure on the right shows the percentage of available data at each height. Since more than 50% of the data are usable for a height region below 22–23 km, characteristics observed in the vertical profile up to this height are certainly reliable.

There are two possible reasons of the vertical variation of the power of VWDs observed in the active periods: one is the change in structure such as the aspect ratio of a vertically propagating wave due to the vertical variation of the background horizontal wind, and the other is superposition of several localized waves. These possibilities can occur coincidentally. In order to investigate this issue, we examine the vertical structure of the VWDs in more detail through spectral and correlation analyses in the following sections.

a. Height distribution of power spectra

The energy content power spectra of w for the active periods are shown as a function of height in Fig. 4. The FFT (Fast Fourier Transform) method was used for calculation of power spectra. Missing data were interpolated with a linear method. However, the spectra should be correctly estimated at least for the height range of 5–22 km, which has a high percentage of usable data as described before (see Fig. 3). The spectra were smoothed by lowpass filters with cutoff lengths of 15 data points (2.25 km) for height and 10 (for B, C) or

20 (for D_2) spectral points for frequency. For the data with finite observational periods, the frequency range that can be examined statistically by spectral and correlation analyses is restricted. Thus, the investigation is made for the components having periods less than one-fifth of the observation period.

It is found that the three maps of spectra have several common features: large power is observed at periods of longer than 0.5 h, and the power decreases sharply around a height of 19–20 km at almost all periods. The decrease of power is clearly shown by line plots of the power spectra (Fig. 5). The scales for B, C, and D_2 are shifted a factor of 10 to distinguish one from the other. This figure indicates that the decrease at 20 km is especially large at periods longer than 1 h (where the power is large). Fritts and VanZandt (1987) showed that the shape of frequency spectra for gravity waves is modified by the Doppler effect of the background wind. However, the large power decrease observed in Figs. 4 and 5 cannot be explained since the Doppler effect does not change the total power. Thus, the change in power and shape of the spectra at 20 km must have another meaning.

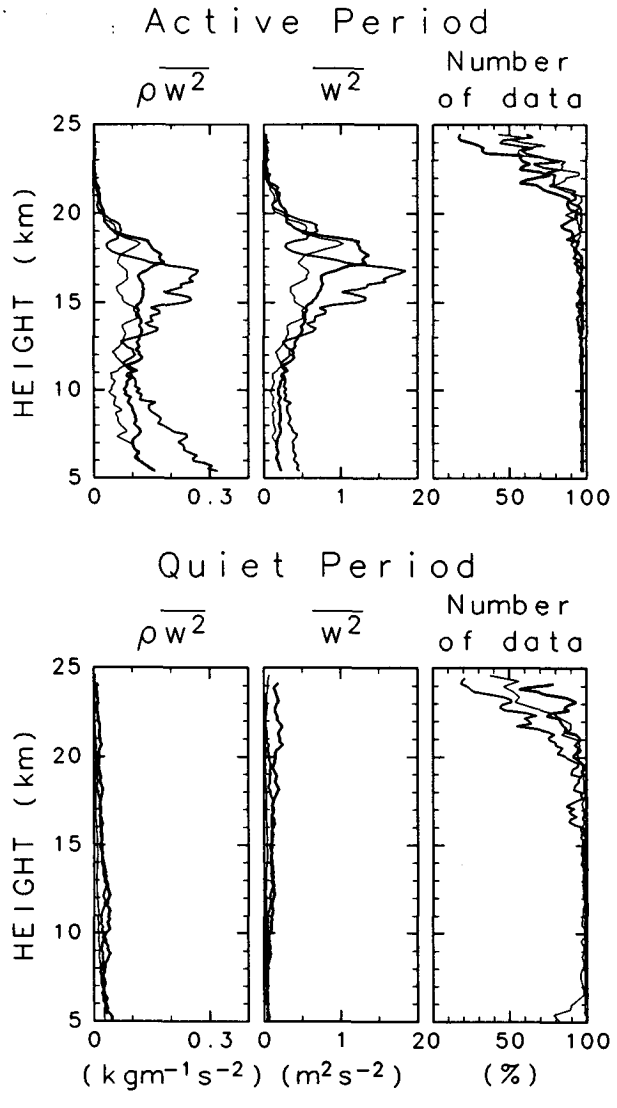

FIG. 3. Vertical profiles of the variance of vertical wind velocity (middle) and those weighted (left) by air density for active (top) and quiet (bottom) periods. Right figures show the percentage of available data at each height. The curve types are as in Fig. 2.

Ecklund et al. (1985) pointed out from the measurements with clear-air Doppler radars in Rhone Delta, France, during ALPEX that the frequency spectra of w are in the shape of $\omega^{-5/3}$ for active periods, while those for quiet periods are proportional to ω^0. Moreover, Ecklund et al. (1986) showed that the general shape of spectra for quiet periods is also observed at other stations, such as, Poker Flat, Alaska; Platteville, Colorado; and Ponape, Micronesia. From the fact that spectra of horizontal wind component were often observed in the shape of $\omega^{-5/3}$ (e.g., Balsley and Carter 1982), they attributed the shape of w spectra for active periods to "horizontal" motions along sloping isentropic surfaces that were constructed by severe topographic waves. However, they did not give the mechanism for the "horizontal" motions.

For comparison three straight lines showing inclination of $\omega^{-5/3}$ in the power-content plots were drawn in Fig. 5. For the w spectra below 20 km where large fluctuations were seen, the inclination of each power spectrum is large but not necessarily $\omega^{-5/3}$, and not constant over the whole frequency range. In particular smaller power is observed in D_2 at frequencies less than $(3\text{ h})^{-1}$. This suggests that the explanation of the "horizontal" motions is not appropriate for the spectra shown in Fig. 5.

b. Correlation among different heights

In this section we investigate the vertical correlation of the VWDs, which have vertical variations like those shown in Fig. 3. We make an analysis of cross correlation for time series including all components with periods less than one-fifth of the observational period. Such an analysis is important because the VWDs are not dominant at a single frequency but are distributed over a broad frequency range. Since the VWDs seem to be in phase at least for a few kilometers at lower heights (Fig. 1), the time series were averaged in altitude over 1.2 km for a height range below 15 km, 0.6 km for 15–18 km, and 0.3 km for above 18 km.

Contour maps of the cross correlation coefficient for the active periods are shown as a function of height in Fig. 6. Different types of lines indicate the coefficient for different reference heights where the peaks of power were observed (Fig. 3). Positive time lag shows the progression relative to w at the reference height. From the figure it is found that the height region with large correlation coefficients spans about 8–9 km at the maximum, that the VWDs keep high correlation for

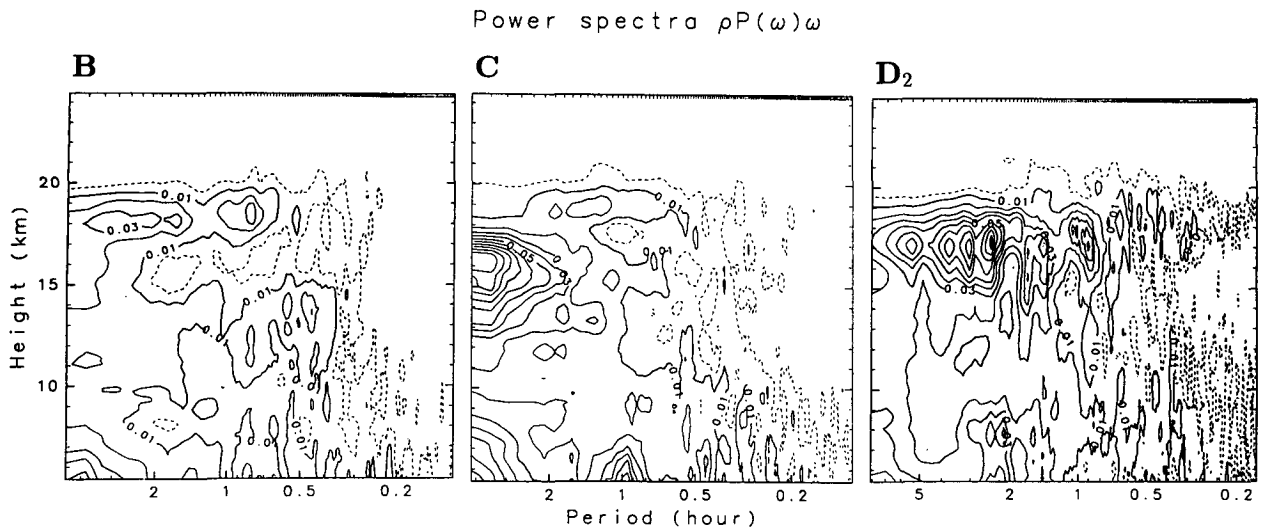

FIG. 4. Vertical profiles of power frequency spectra of vertical wind weighted by air density for each active period in the energy-content form. The interval of the solid contour line is 1×10^{-2} (kg m^{-1} s^{-2}) and the dotted contour line shows 0.5×10^{-3} (kg m^{-1} s^{-2}). Tick marks on the upper frequency axis show the locations of spectral points.

as long as 0.5–1.5 h, which is also expected from the spectral analysis, and that correlation at each height is greatest at small lag. These facts indicate that the phase of VWDs is almost vertical over a large vertical expanse.

It is also important that the high correlation is not observed in the whole height region below 20 km where the power of vertical wind is large, and that the correlation time depends on the reference heights. We infer from the features that the VWDs do not consist of one mode.

In order to make this point clear, the distribution of the maximum cross correlation coefficient for w's at each pair of heights (H_{ref}, H_i) is examined. The correlation map for case B is shown in Fig. 7. There are some narrow parts around the dotted line of $H_i = H_{\text{ref}}$, namely at 10, 16, and 19 km. This suggests that several mutually independent modes exist in different height regions with boundaries indicated by the narrow parts. Similar features were observed for the other active periods of C and D_2. We, therefore, deduce that the VWDs are composed of several modes dominating at different heights and frequencies.

It is also significant that little correlation is observed above 20 km for any lower reference heights. These features are also seen for C and D_2. This indicates that variations in w above 20 km are not only small, but also have little correlation with large variation in w at the lower heights in the active periods.

c. *Interpretation of a level of 20 km*

Results obtained by the spectral and correlation analyses show that the height of 20 km is a special level for the VWDs, such as a critical level. As shown in Fig. 2, the horizontal wind has a similar profile in the active

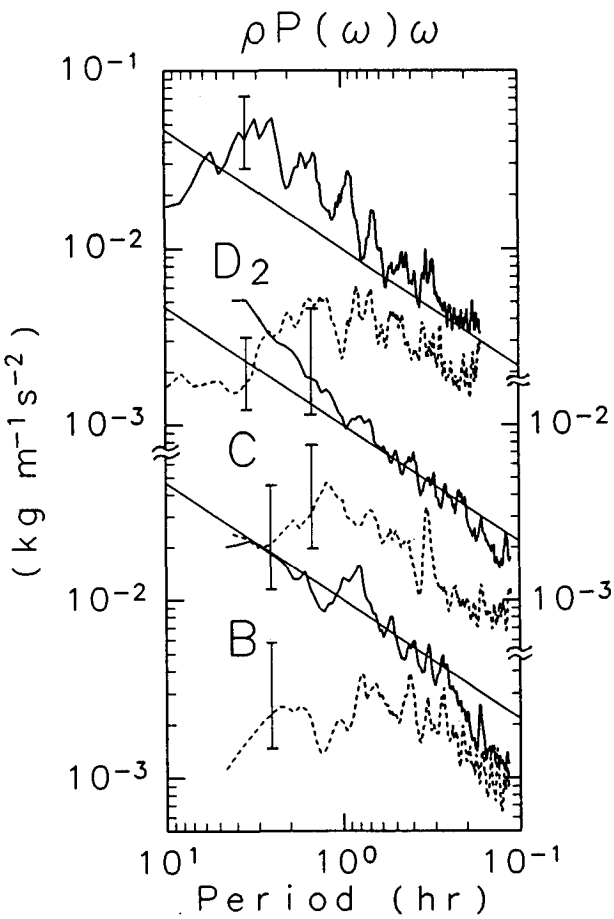

FIG. 5. Power spectra of vertical wind weighted by air density in the energy content form for each active period. Solid and dotted lines show the average for height ranges of 5–20 km and 20–22 km, respectively. Lines showing $\omega^{-5/3}$ are included for comparison. Error bars show confidence intervals of 95%.

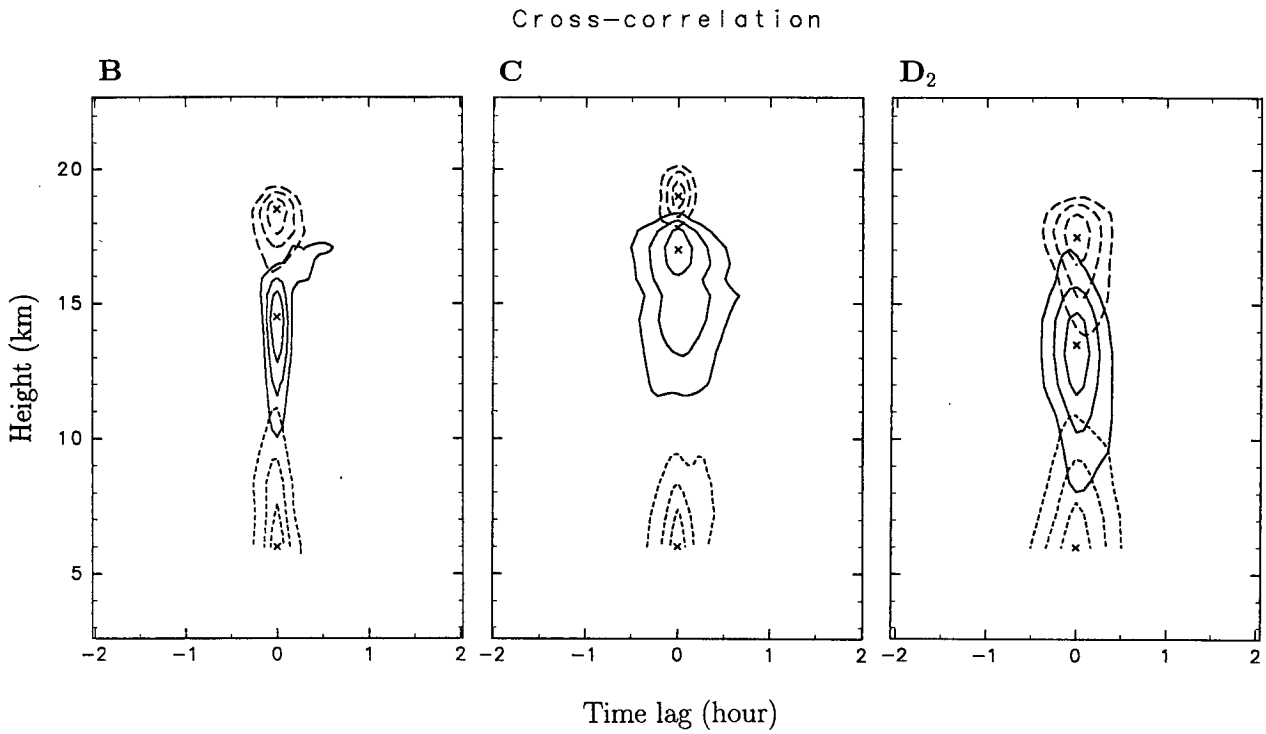

FIG. 6. Cross-correlation coefficient of time-series of the vertical wind for each active period. Different contour lines show the profiles with different reference heights, which are presented by '×'. Contour lines are drawn at an interval of 0.2 with the minimum value of 0.4.

periods: a peak at ~11 km and decrease above the height to a small value of several meters per second at 20 km. Thus, if a critical level of the VWDs is located at 20 km, the VWDs have small horizontal phase velocities corresponding to the horizontal wind there. This is consistent with a view that the VWDs observed with the MU radar are also due to gravity waves generated by topographic effects as suggested by Ecklund et al. (1982). It is noteworthy that the decrease of the power at ~20 km was seen in a wide range of frequency. This suggests that the components of the VWDs with high frequencies are also due to topographically-forced waves. We deduce, therefore, that the frequencies that appear in the spectra do not indicate "frequencies" of respective "waves," but show a feature of "spatial phase modulation" of the topographic waves by temporal variation of the background wind.

Some other features on the structure of the VWDs described above can also be interpreted well as characteristics of topographically forced waves. The distribution of large power at small frequencies is consistent with the view of mountain waves. Large vertical scales of the VWDs shown by the cross correlation analysis would correspond to the large vertical wavelength of mountain waves.

It should be noted here that Ohno (1988) showed a strong turbulent layer around a height of 18–19 km from profiles of echo power and spectral width of the echo in an active period of D_2 (Fig. 8), which is similar to a severe turbulent layer associated with mountain waves detected by aircraft (Lilly and Kennedy 1973).

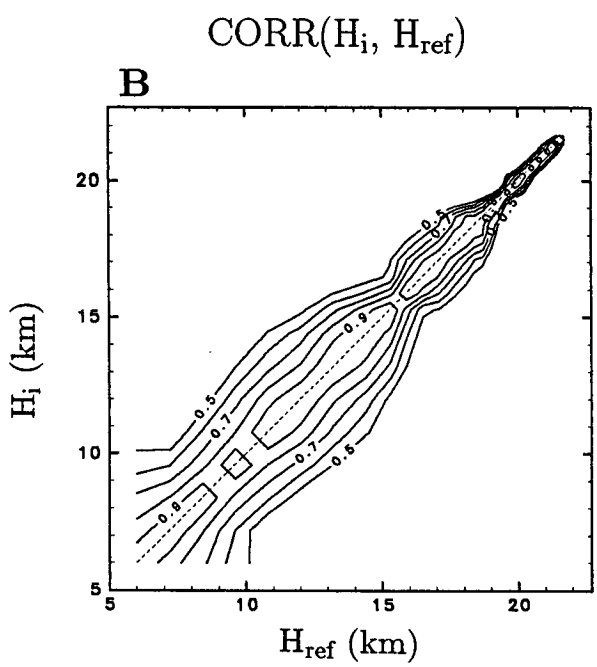

FIG. 7. The maximum vertical cross-correlation coefficient at a height of H_i for the reference height H_{ref} in the case of B.

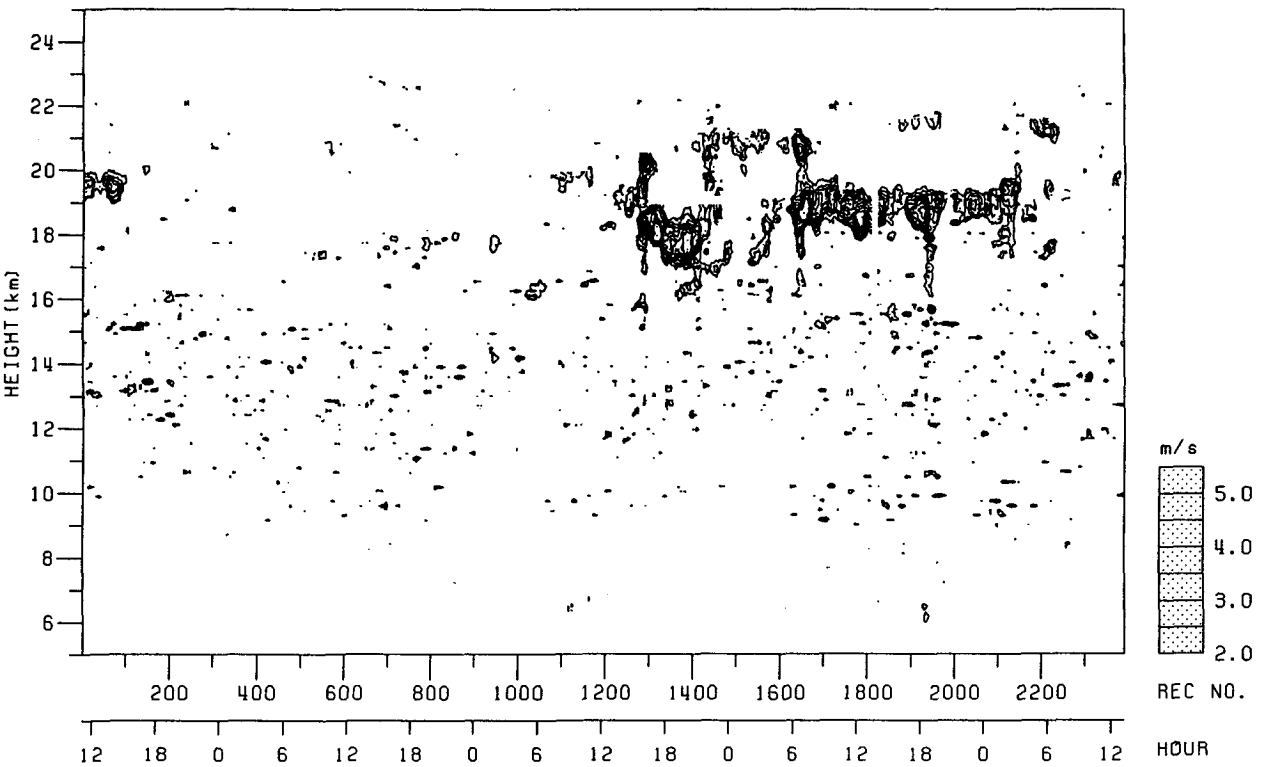

FIG. 8. Vertical time section of spectral width of echo obtained in the observational period D. The spectral broadening due to the effect of finite beam width of the radar was removed from the original spectral width (Hocking 1983) (after Ohno 1988).

Such strong turbulent layers are also observed in other active periods B and C (not shown). This implies that the mountain waves propagate upward toward the critical layer increasing their amplitudes, but break due to occurrences such as convective instability before reaching the critical layer.

5. Correlation between vertical wind activity and horizontal wind near the surface

Ecklund et al. (1982) deduced that VWDs observed in the lee of the Colorado Rockies are generated due to the topographic effect, from the high correlation between the power of VWDs and the horizontal wind at 500 mb, and from the fact that larger power of the VWDs was observed nearer mountains. We have discussed through the previous analyses that several features of the VWDs observed with the MU radar are consistent with the view of mountain waves. However, there is no decisive evidence showing that the VWDs observed with the MU radar are due to topographically-forced waves. Around the MU radar site (Shigaraki), westerly wind is dominant in late autumn and winter when the VWDs appear, whereas there are no high mountains within a distance of 100 km west of Shigaraki, as shown in a map of topography (Fig. 9). Mountains higher than 1000 m are located at a long distance of 150–200 km. If VWDs observed at Shigaraki are caused by the topographic effect, the correlation with horizontal wind near the surface should be high at locations west of the mountains.

Thus, we examine horizontal wind at Yonago denoted by '□' in Fig. 9, where routine balloon observations are made every 00Z and 12Z by the Japan Meteorological Agency. As an index of vertical wind activity, we employ the time and vertical mean square of vertical wind fluctuations for eight hours around 00Z and 12Z and for a height range of 5–20 km at Shigaraki. Using a threshold index value of 0.16 m^2 s^{-2}, 13 active and 14 quiet periods are obtained for eight observations shown in Table 1. Figure 10(a) represents horizontal wind vectors at 900 mb (~1 km) observed at Yonago, which are categorized as active and quiet periods by symbols of '*' and 'O,' respec-

tively. It is obvious that the wind vectors for active periods are distributed in a confined region of Fig. 10(a), which shows large dependence on direction as well as strength. The dependence does not change when different threshold values for activity index are used. The correlation between horizontal wind at Yonago and vertical wind activity at Shigaraki becomes lower at higher altitude. For example, wind vectors at 600 mb (~4 km) are shown in Fig. 10(b). It is noteworthy that the wind vectors at 900 mb for active periods are directed toward Shigaraki (see Fig. 9) and that there is a mountainous area confined along the line between Yonago and Shigaraki.

Similar analyses were made for Wajima and Shionomisaki, which are located at a distance of ~300 km northeast and ~150 km south of Shigaraki, respectively. Figure 11 shows the horizontal wind vectors at 900 mb for each station. High correlation as seen at Yonago is not observed. This suggests that the appearance of the VWDs is controlled by a local wind field between Yonago and Shigaraki.

Figure 12 presents a synoptic chart at 850 mb for an active period where high correlation of vertical wind activity with horizontal wind at Yonago is also observed. Yonago and Shigaraki are on the same contour of geopotential height, indicating that Yonago is windward of Shigaraki. A similar feature is also observed in synoptic charts at the other active periods.

These relationships between lower tropospheric winds and VWDs imply that the VWDs observed in late autumn and winter by the MU radar are forced by mountains located between Yonago and Shigaraki.

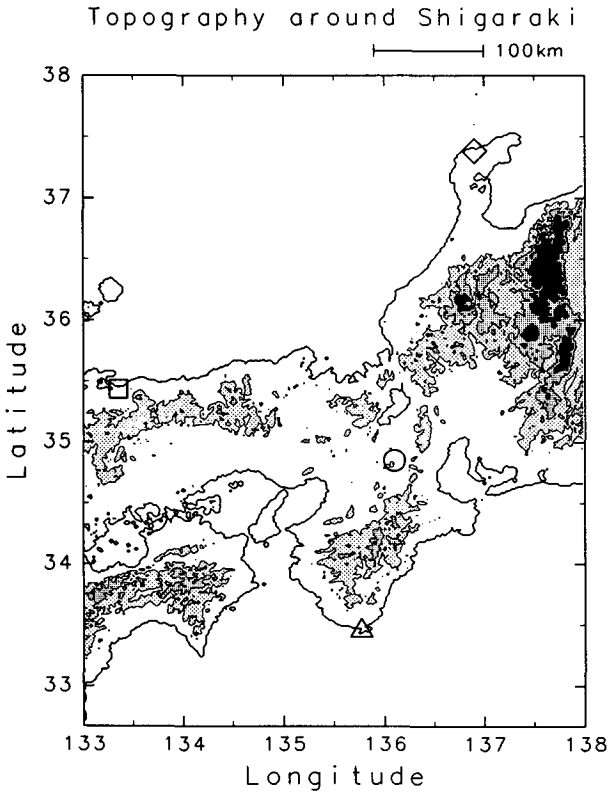

FIG. 9. Map of topography around the MU radar site, Shigaraki (○). Yonago, Wajima, and Shionomisaki are represented by □, ◇, and △, respectively.

6. Vertical momentum flux in the active periods

The divergence of vertical momentum flux is important when studying interaction between small-scale disturbances like gravity waves and atmospheric motions with synoptic and/or planetary scales (e.g., Fritts 1984). Moreover, if the disturbances are due to gravity waves, the vertical momentum flux is also valuable for investigation into their characteristics.

For two-dimensional gravity waves assuming u', $w' \propto \exp^{i(kx+mz-\omega t)}$, the continuity equation under the Boussinesq approximation becomes

$$ku' + mw' = 0, \tag{1}$$

where ω is observed frequency and the other notations are as usual. Equation (1) holds for three-dimensional waves if x is chosen parallel to the horizontal wavenumber vector. Using (1) the vertical momentum flux is expressed as

$$\overline{u'w'} = -k\overline{u'^2}/m, \tag{2}$$

where the overbars denote the spatial and temporal mean. When the intrinsic frequency $\hat{\omega}$ is restricted to the positive without losing any generality, the wave propagating energy upward will have negative m (e.g., Hirota and Niki 1985). Thus the direction of the horizontal wavenumber vector of gravity waves propagating upward is deduced from the sign of vertical momentum flux using (2) as

$$\left.\begin{aligned} \overline{u'w'} > 0 \quad \text{for} \quad k > 0 \\ \overline{u'w'} < 0 \quad \text{for} \quad k < 0 \end{aligned}\right\}. \tag{3}$$

In the case of stationary mountain waves excited in the westerly wind $\bar{u}$ (>0), the intrinsic phase speed $\hat{c} = \hat{\omega}/k$ is related to $\bar{u}$ as

$$\hat{c} = -\bar{u}. \tag{4}$$

This means that the zonal wavenumber k is negative, and hence (3) suggests that the zonal component of the vertical momentum flux should be negative.

a. Method of estimation of vertical momentum flux by the VHF radar observations and its application to the VWD events

Vincent and Reid (1983) showed a method of estimation of the vertical momentum flux using wind data obtained with the VHF radar observations. The

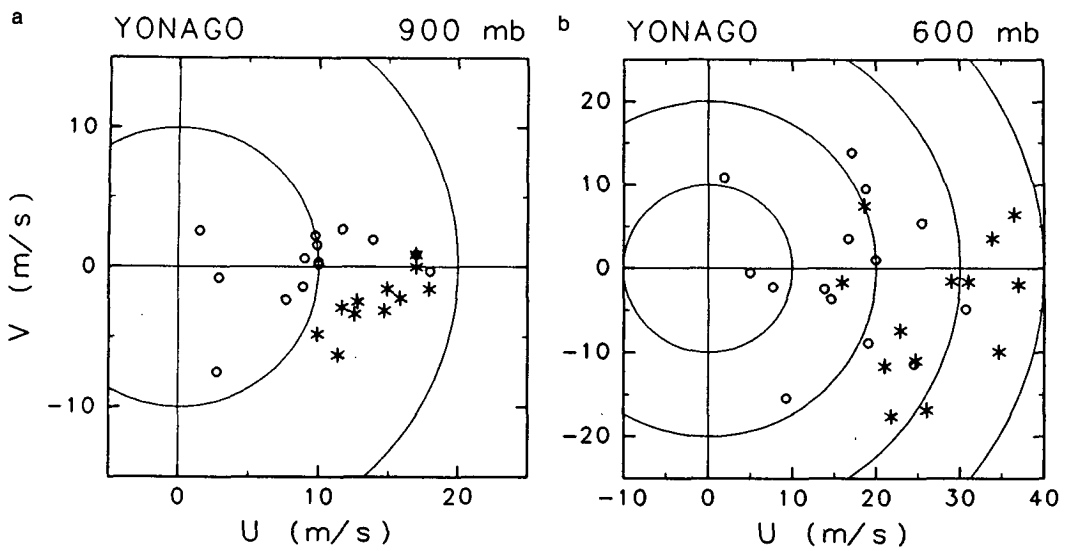

FIG. 10. Scatter diagram between vertical wind activity index at Shigaraki and horizontal wind at Yonago at (a) 900 mb and (b) 600 mb. The activity index is defined as the time and vertical mean square of vertical wind fluctuations for 8 hours around 00Z and 12Z and for a height range of 5–20 km. The horizontal wind vectors when the activity index is more than and less than 0.16 $m^2 s^{-2}$ are shown by * and O, respectively.

vertical momentum flux is obtained from the difference between mean squares of the line-of-sight (radial) velocities measured by two beams tilted with equal and opposite angles $\pm\theta$ around the zenith, under an assumption of a homogeneous field of disturbances. However, this method cannot be used for estimation of vertical momentum flux associated with quasi-stationary waves. It is difficult to extract the wave components from the wind data using any filter for time and/or height, because the waves have similar time and vertical scales to the background wind.

It should be noted, however, that the VWDs have large temporal fluctuations with high frequencies. As discussed in section 4 the observed frequencies show phase modulation of mountain waves by variation of the background wind. If the temporal fluctuation of phase is sufficiently large, we can estimate vertical momentum flux associated with the mountain waves by

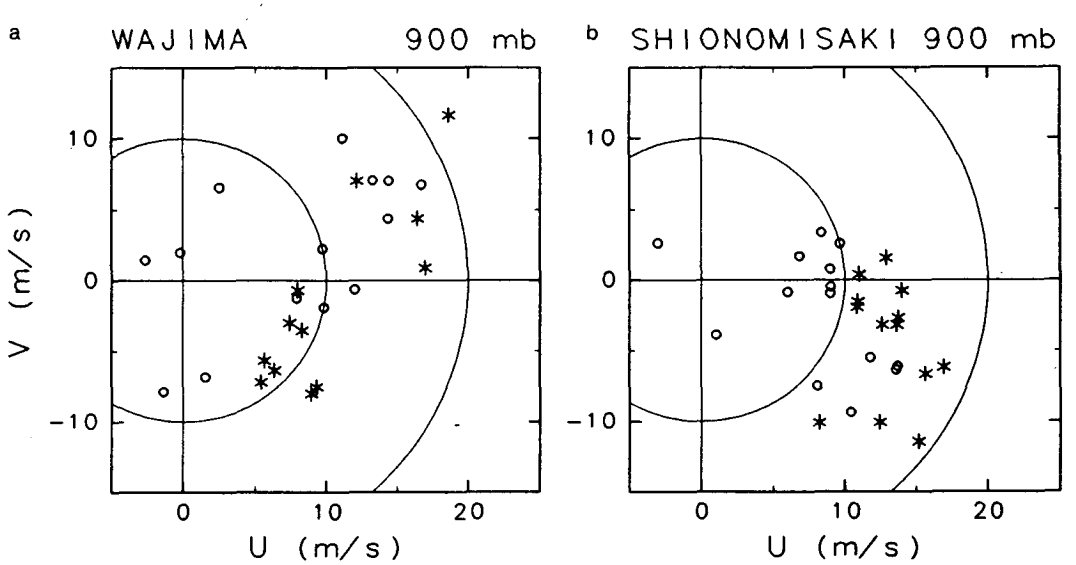

FIG. 11. The same as Fig. 12 but for 900 mb at Wajima and Shionomisaki.

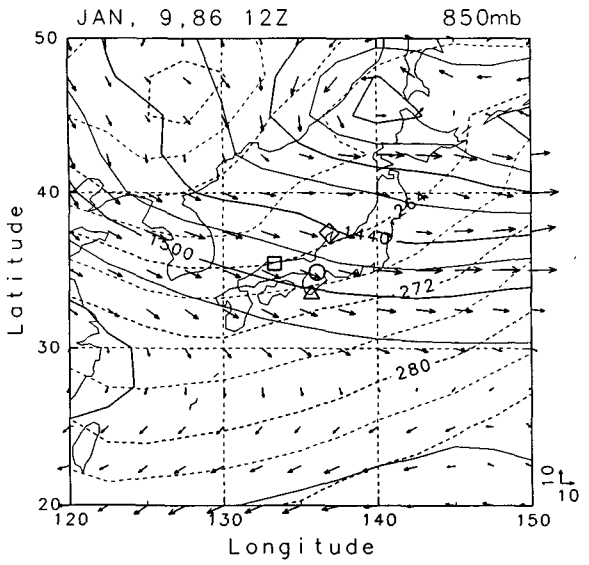

FIG. 12. A synoptic chart at 850 mb at an active period of D_2 (21 LST 9 Jan 1986). Contours of geopotential height are continuous. Temperature contours are dashed. Vectors show horizontal winds. Unit vectors indicate zonal and meridional winds of 10 m s^{-1}, respectively. Shigaraki, Yonago, Wajima, and Shionomisaki are denoted by O, □, ◇, and △, respectively.

replacing spatial average with time average; i.e., the Vincent and Reid's method can be applied to the VWD events under an assumption that the phase passing occurs equally at the two symmetrical beam positions instead of assuming homogeneous field of disturbances. It is found from Figs. 2 and 3 that vertical wind fluctuations are very large compared with the mean vertical wind. This suggests significance of the analysis using a time filter for vertical momentum flux associated with the VWDs.

In this study, the vertical momentum flux is examined as a function of frequency. The method of calculation for the frequency spectra of vertical momentum flux is an expansion of the method shown by Vincent and Reid. We use power spectra of radial velocities obtained by two symmetrical beams around the zenith instead of the mean squares. Detailed description about the method is given in the Appendix. This method is useful for cases when a lot of gravity waves with different frequencies are observed simultaneously. The observed frequency of a wave is invariant during propagation when the background wind has no temporal variation (Lighthill 1978). Thus, we can investigate separately the vertical propagation of respective gravity waves with different frequencies through examination of vertical profiles of the frequency spectra of vertical momentum flux, if the wave periods are much smaller than the time-scale of change in the background wind. In the case of the VWDs, such examination is impossible because frequencies observed in the wind data are not corresponding to those of gravity waves. However, comparison in characteristics between the spectra of vertical momentum flux and the power spectra examined in section 4 is meaningful. We can examine through such comparison whether the obtained vertical momentum flux is related to the VWDs.

b. Profiles of vertical momentum flux

For the calculation of power spectra of radial velocities, the Blackman–Tukey method is used because of the existence of missing values. Auto correlation function is obtained with the maximum lag of one-fourth of the observational period. Power spectra are estimated for heights where the number of data usable for calculation of the auto correlation at every time lag is more than 30% of the total number of data. In order to avoid the mixing of components other than the VWDs, we use the data smoothed in height with a low-pass filter with a cutoff length of 2.25 km, since the VWDs have large vertical scales as shown by the correlation analysis (Fig. 6).

First, we examine the difference in vertical momentum flux between the active and quiet periods for period D. Figure 13 shows the vertical profiles of frequency spectra of the vertical momentum flux weighted by air density in a flux-content form for the active and quiet periods. Only components having shorter periods than one-fifth of the observation period are plotted as in the power spectral analysis (section 4). Compared with the quiet period, large momentum flux is observed in both zonal and meridional components in the active period.

The momentum flux in the active period is not uniform from bottom to top, but is divided into several parts by height. This is in accord with the result in section 4 that the VWDs consist of several modes dominating in different height regions. An important feature observed in Fig. 13 is that large westward momentum flux above the westerly jet vanishes at almost all frequencies around 19 km corresponding to the height where the w power sharply decreases. This indicates that momentum deposition from the VWDs to the background wind may occur there, which is consistent with characteristics of a critical level. It is worth noting that the vertical momentum flux has a directional tendency. In a height range above 15 km, where a large power of vertical wind fluctuation exists (Fig. 3), the zonal components are biased toward negative at almost all frequencies (except for around a period of 3 h), whereas the meridional components are distributed evenly between positive and negative values. This suggests that the VWDs have totally negative zonal component of the vertical momentum flux, which accords with the view of mountain waves excited in the westerly wind. These characteristics on the momentum flux are also found for the other active periods of B and C except the sign of the zonal components below ~20 km, which is positive for B and negative for C

(not shown). The positive value for B is hard to be explained by the mountain waves generated in the westerly wind and propagating upward. Thus, the other physical explanation is necessary such as reflection from the critical level. However, this is beyond the scope of this study since we cannot get sufficient in-

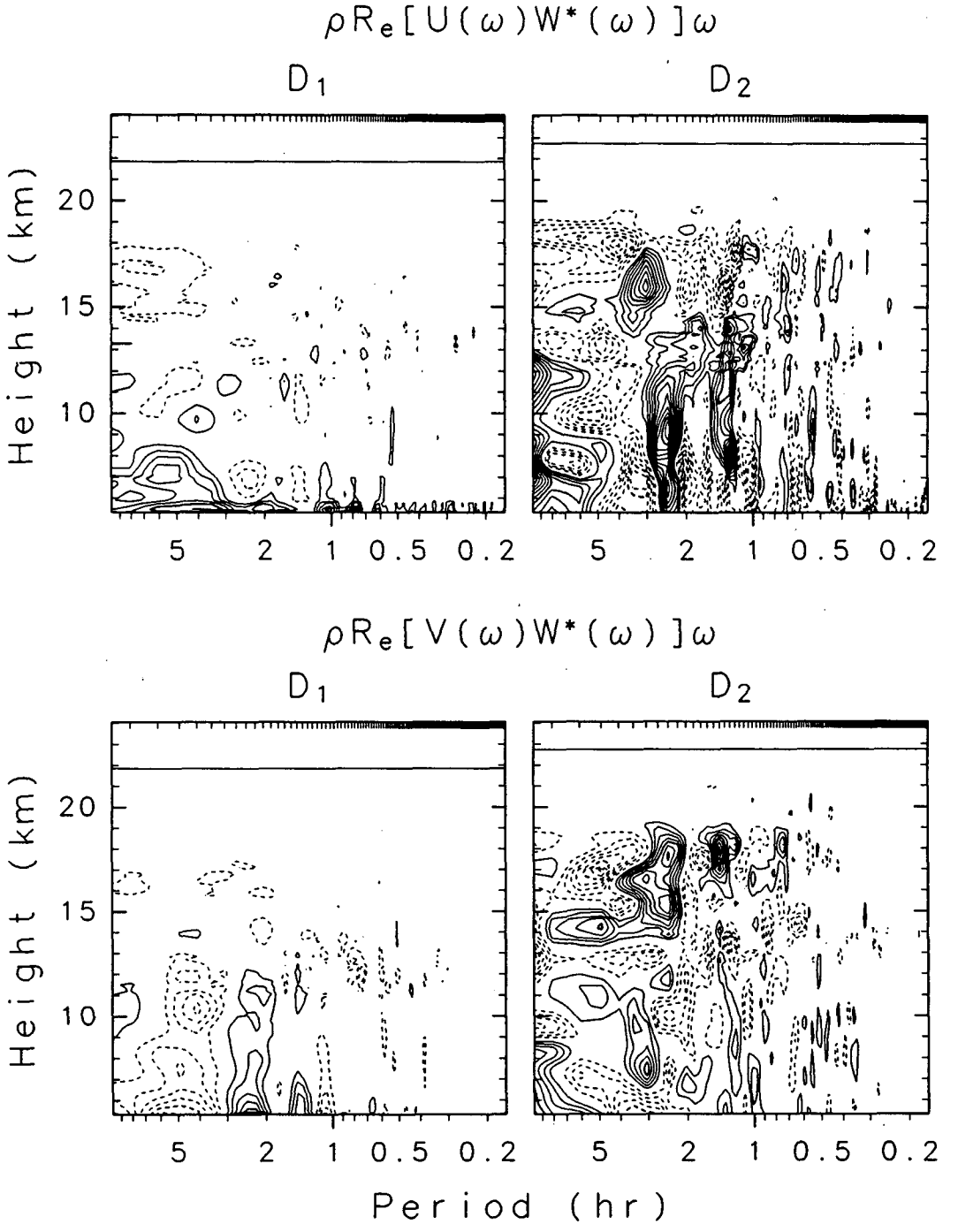

FIG. 13. Vertical profiles of zonal (top) and meridional (bottom) components of vertical momentum flux as a function of frequency in the flux-content form, for active (right) and quiet (left) periods for case D. Solid and dotted lines show positive and negative values, respectively. Contour interval is 1.5×10^{-2} (kg m^{-1} s^{-2}). The zero contour is omitted. The straight horizontal lines indicate the heights above which the estimation could not be made owing to missing data. Tick marks on the upper axis show the locations of spectral points.

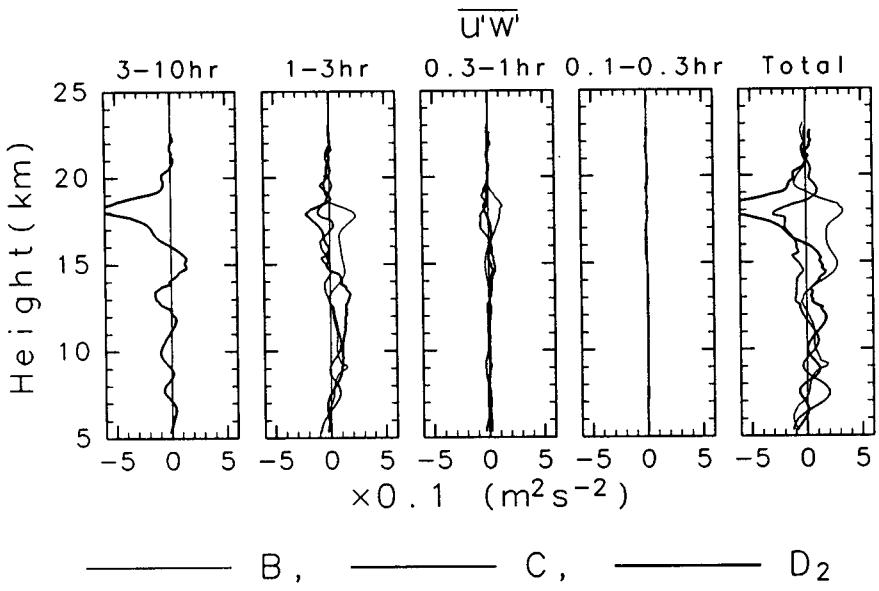

FIG. 14. Vertical profiles of zonal components of vertical momentum flux for the period ranges of 0.1–0.3, 0.3–1.0, 1–3, and 3–10 hrs for the active periods of B (very thin line), C (thin line), and D_2 (thick line). "Total" profiles are obtained by adding components with periods less than (the observation period)/5.

formation from the present data that is necessary for the investigation.

Next, the detailed frequency dependence versus height is examined for the active periods. The frequency range is divided into quarters, namely, 3–10, 1–3, 0.3–1.0, and 0.1–0.3 hours (same length on log scale), and the spectra of vertical momentum flux are summed for each of the divided frequency ranges. Figure 14 shows the profiles of zonal components for the frequency ranges and a total. Note that the "total" profiles were obtained by adding up the components not for the divided frequency ranges, but for the frequencies more than (observation period)$^{-1} \times 5$; i.e., 0.1–4.0 h for B and C, and 0.2–10.0 h for D_2, for which statistically meaningful analysis is possible. The different types of lines show different observation periods. In any case of the active periods, larger momentum flux is observed in the lower frequency ranges, which resembles the frequency distribution of w-power. Similar distribution in frequency ranges are observed also for meridional components (not shown). The "total" vertical momentum flux found in Fig. 14 amounts to about 0.3–0.5 $m^2 s^{-2}$ ($\sim$0.03–0.05 kg $m^{-1} s^{-2}$) at upper levels. The momentum flux shown here is not weighted by air density, because the accuracy is independent of height. The accuracy of vertical momentum flux ($\overline{u'w'}$) corresponding to the radial wind velocity resolution of 0.1 m s^{-1} is 0.015 $m^2 s^{-2}$ [$0.1^2/2 \sin(2 \times 10°)$]. Thus the estimated value is significant.

Some observational studies of stationary mountain waves using aircraft detected large vertical momentum flux with a decrease in the lower stratosphere (e.g., Lilly and Kennedy 1973; Lilley et al. 1982; Brown 1983; Hoinka 1984, 1985), and they are summarized concisely in Palmer et al. (1986). According to these studies, the magnitude of vertical momentum flux is 0.05–1.2 kg $m^{-1} s^{-2}$, depending on the intensity of mountain waves. The vertical momentum flux of about 0.03–0.05 kg $m^{-1} s^{-2}$ obtained for active periods in this study is comparable to or less than those of the earlier studies. However, it must be noted that the estimation made in this study is restricted to components having periods less than the observational period. Thus, more quantitative discussion cannot be made. Wavelike structure appearing in the vertical profile of the momentum flux may show limitation of validity of the assumption that phase modulation is large enough to replace the spatial average for $u'w'$ with the time average. The wavelike structure is probably due to the vertical wavelength of mountain waves ("wavelength" of vertical variation of the vertical momentum flux is half the vertical wavelength of mountain waves because the vertical momentum flux is a quadratic value). The limitation of assumption can be compensated to some extent by the vertical average. Thus the vertically smoothed momentum flux is still meaningful.

7. Conclusion

VWDs observed in late autumn and winter with the MU radar were examined. Several interesting aspects of three cases of VWDs were found in the vertical dis-

tribution of power spectra and correlation in the height direction. The characteristics are well explained if the VWDs are due to topographically forced gravity waves whose phases are fluctuating due to temporal changes of the background wind. High correlation between lower-level horizontal winds obtained by routine balloon observations at some locations and the vertical wind activity observed with the MU radar supports the interpretation. Vertical momentum flux $u'w'$ is examined under an assumption that the spatial average for $u'w'$ associated with the mountain waves can be replaced with the time average of $u'w'$ observed with the MU radar. As a result, it is found that large momentum flux is associated with the VWDs, and that the distribution in a height-frequency space is similar to the power. The obtained vertical momentum flux is consistent with the previous studies on the mountain waves except the sign at one case out of three of the VWDs. However, the dominance of positive zonal components of the vertical momentum flux in the one case is still an open question. Long term observations of the VWDs are necessary to confirm this issue.

Examination of the frequency of appearance of the VWDs will help us to understand the significance of VWDs for wind systems with long time scales in the lower stratosphere. It is also necessary to statistically confirm the results obtained in this study through similar analyses for several other active periods. The effort to detect parameters of the VWDs, such as horizontal wavelength, that have not yet been estimated is important because they provide some valuable information for understanding the nature of the VWDs in the background wind. Sato and Hirota (1988) made a multibeam observation using the MU radar to directly estimate small horizontal wavelengths of some coherent waves that dominate the vertical wind component. Carter et al. (1989) also directly detected the horizontal wavelength of some coherent waves through the measurements of vertical wind using three closely spaced wind profilers. Since the VWDs also have small horizontal scales, further observations by multibeams are promising in the future.

Acknowledgments. The author would like to thank Prof. I. Hirota for fruitful discussion and encouragement, and Drs. T. Tsuda, T. Sato, and M. Yamada for their helpful comments. Thanks are also due to Dr. E. Fetzer for his critical reading and comments on the original manuscript. K. Sato is grateful to the staff members of the Radio Atmospheric Science Center of Kyoto University for technical advice on performing the measurements by the MU radar. The author wishes to thank Messrs. T. Niki and Y. Ohno and Prof. S. Fukao because some of the data used in this study were obtained through the measurements made by them. The MU radar belongs to and is operated by the Radio Atmospheric Science Center of Kyoto University.

APPENDIX

Calculation Method of Frequency Spectra of Vertical Momentum Flux

The frequency spectra of vertical momentum flux is obtained with an expanded method of that proposed by Vincent and Reid (1983). Vincent and Reid showed that the vertical momentum flux is obtained from the difference between mean squares of the line-of-sight (radial) velocities measured by two beams tilted with equal and opposite angles $\pm\theta$ around the zenith in the following way. Radial wind velocities $V_{\pm\theta}$ obtained using the symmetrical beams are expressed as

$$V_{\pm\theta} = \pm u \sin\theta + w \cos\theta, \tag{5}$$

where u and w are the horizontal and vertical wind components. Since the mean squares of the radial components of disturbances $\overline{V'^2_{\pm\theta}}$ are

$$\overline{V'^2_{\pm\theta}} = \overline{u'^2} \sin^2\theta + \overline{w'^2} \cos^2\theta + \overline{u'w'} \sin 2\theta, \tag{6}$$

where u' and w' are horizontal and vertical components of the disturbances, respectively, and the vertical momentum flux is estimated as

$$\overline{u'w'} = \frac{\overline{V'^2_{\theta}} - \overline{V'^2_{-\theta}}}{2 \sin 2\theta}. \tag{7}$$

This method assumes that the field of disturbances is homogeneous over the spatial region between the two beam positions. This assumption is thought to be generally satisfied when the beams are only tilted with a sufficiently small zenith angle. Studies have shown that Vincent and Reid's method provides good estimates of vertical momentum flux compared with the other methods where homogeneity of wind between beams is assumed (Reid 1987; Fukao et al. 1988).

The present method makes use of two frequency power spectra of radial velocities obtained by the symmetrical beam pair instead of the mean squares. The two power spectra of the radial velocities, $P_{V_{\pm\theta}}(\omega)$, are expressed as,

$$P_{V_{\pm\theta}}(\omega) = U(\omega)U^*(\omega) \sin^2\theta + W(\omega)W^*(\omega) \cos^2\theta \pm \mathrm{Re}[U(\omega)W^*(\omega)] \sin 2\theta, \tag{8}$$

where ω is observed frequency, $U(\omega)$ and $W(\omega)$ are Fourier components of horizontal and vertical velocities, respectively, and $U^*(\omega)$ and $W^*(\omega)$ show the complex conjugates. The term $\mathrm{Re}[U(\omega)W^*(\omega)]$ in (8) shows the vertical momentum flux associated with gravity waves having a frequency of ω, which is calculated immediately from (8):

$$\mathrm{Re}[U(\omega)W^*(\omega)] = \frac{P_{V_{+\theta}}(\omega) - P_{V_{-\theta}}(\omega)}{2 \sin 2\theta}. \tag{9}$$

The total vertical momentum flux is obtained from the spectra:

$$\overline{u'w'} = \sum_{\omega} \mathrm{Re}[U(\omega)W^*(\omega)]. \qquad (10)$$

Similarly, we can obtain not only the spectra of zonal and meridional components of the vertical momentum flux but also the power spectra of three wind components, from the power spectra of five radial velocities measured using five beams tilted to east, west, north, and south, and directed vertically.

REFERENCES

Balsley, B. B., and D. A. Carter, 1982: The spectrum of atmospheric velocity fluctuations at 8 km and 86 km. *Geophys. Res. Lett.*, **9,** 465–468.

Brown, P. R. A., 1983: Aircraft measurements of mountain waves and their associated flux over the British Isles. *Quart. J. Roy. Meteor. Soc.*, **109,** 849–866.

Carter, D. A., B. B. Balsley, W. L. Ecklund, K. S. Gage, A. C. Riddle, R. Garello and M. Crochet, 1989: Investigations of internal gravity waves using three vertically directed closely spaced wind profilers. *J. Geophys. Res.*, **94,** 8633–8642.

Ecklund, W. L., K. S. Gage and A. C. Riddle, 1981: Gravity wave activity in vertical winds observed by the Poker Flat MST radar. *Geophys. Res. Lett.*, **8,** 285–288.

——, ——, B. B. Balsley, R. G. Strauch and J. L. Green, 1982: Vertical wind variability observed by VHF radar in the lee of the Colorado Rockies. *Mon. Wea. Rev.*, **110,** 1451–1457.

——, B. B. Balsley, D. A. Carter, A. C. Riddle, M. Crochet and R. Garello, 1985: Observation of vertical motions in the troposphere and lower stratosphere using three closely spaced ST radars. *Radio Sci.*, **20,** 1196–1206.

——, K. S. Gage, G. D. Nastrom and B. B. Balsley, 1986: A preliminary climatology of the spectrum of vertical velocity observed by clear-air Doppler radar. *J. Climate Appl. Meteor.*, **25,** 885–892.

Fritts, D. C., 1984: Gravity wave saturation in the middle atmosphere: A review of theory and observations. *Rev. Geophys.*, **22,** 275–308.

——, and T. E. VanZandt, 1987: Effects of Doppler shifting on the frequency spectra of atmospheric gravity waves. *J. Geophys. Res.*, **92,** 9723–9732.

——, T. Tsuda, T. E. VanZandt, S. A. Smith, T. Sato, S. Fukao and S. Kato, 1990: Studies of velocity fluctuations in the lower atmosphere using the MU radar. Part II: Momentum fluxes and energy densities. *J. Atmos. Sci.*, **47,** 51–66.

Fukao, S., T. Sato, T. Tsuda, S. Kato, K. Wakasugi and T. Makihira, 1985a: The MU radar with an active phased array system, 1. Antenna and power amplifiers. *Radio Sci.*, **20,** 1155–1168.

——, T. Tsuda, T. Sato, S. Kato, K. Wakasugi and T. Makihira, 1985b: The MU radar with an active phased array system, 2. In-house equipment. *Radio Sci.*, **20,** 1169–1176.

——, T. Sato, T. Tsuda, S. Kato, M. Inaba and I. Kimura, 1988: VHF Doppler radar determination of the momentum flux in the upper troposphere and lower stratosphere: Comparison between the three- and four-beam method. *J. Atmos. Oceanic Technol.*, **5,** 57–69.

Hirota, I., and T. Niki, 1985: A statistical study of inertia-gravity waves in the middle atmosphere. *J. Meteorol. Soc. Jpn.*, **63,** 1055–1066.

Hocking, W. K., 1983: On the extraction of atmospheric turbulence parameters from radar backscatter Doppler spectra—I. Theory. *J. Atmos. Terr. Phys.*, **45,** 89–102.

Hoinka, K. P., 1984: Observation of a mountain wave event over the Pyrenees. *Tellus*, **36A,** 369–383.

——, 1985: Observation of the airflow over the Alps during a foehn event. *Quart. J. Roy. Meteor. Soc.*, **111,** 199–224.

Lighthill, 1978: *Waves in Fluid.* Cambridge University Press, 504 pp.

Lilly, D. K., and P. J. Kennedy, 1973: Observations of a stationary mountain wave and its associated momentum flux and energy dissipation. *J. Atmos. Sci.*, **30,** 1135–1152.

——, and J. M. Nicholls, R. M. Chervin, P. J. Kennedy and J. B. Klemp, 1982: Aircraft measurements of wave momentum flux over the Colorado Rocky mountains. *Quart. J. Roy. Meteor. Soc.*, **108,** 625–642.

Ohno, Y., 1988: Strong vertical wind variability in the troposphere and lower stratosphere observed by the MU radar. M.Sc. thesis, Kyoto University, Kyoto, Japan, 26 pp. [Available from Department of Geophysics, Faculty of Science, Kyoto University, Kyoto 606, Japan.]

Palmer, T. N., G. J. Shutts and R. Swinbank, 1986: Alleviation of a systematic westerly bias in general circulation and numerical weather prediction models through an orographic gravity wave drag parameterization. *Quart. J. Roy. Meteor. Soc.*, **112,** 1001–1039.

Reid, I. M., 1987: Some aspects of Doppler radar measurements of the mean and fluctuating components of the wind field in the upper middle atmosphere. *J. Atmos. Terr. Phys.*, **49,** 467–484.

Sato, K., and I. Hirota, 1988: A small-scale internal gravity waves in the lower stratosphere revealed by the MU radar multi-beam observation. *J. Meteorol. Soc. Jpn.*, **66,** 987–999.

VanZandt, T. E., S. A. Smith, T. Tsuda, D. C. Fritts, T. Sato, S. Fukao and S. Kato, 1990: Studies of velocity fluctuations in the lower atmosphere using the MU radar. Part I: Azimuthal anisotropy. *J. Atmos. Sci.*, **47,** 39–50.

Vincent, R. A., and I. M. Reid, 1983: HF Doppler measurements of mesospheric gravity wave momentum fluxes. *J. Atmos. Sci.*, **40,** 1321–1333.